J Am Oil Chem Soc (2013) 90:1773–1786
DOI 10.1007/s11746-013-2329-6

ORIGINAL PAPER

Crystallization Behavior of High-Oleic High-Stearic Sunflower Oil Stearins Under Dynamic and Static Conditions

S. Martini · J. A. Rincón Cardona · Y. Ye · C. Y. Tan · R. J. Candal · M. L. Herrera

Received: 17 September 2012 / Revised: 19 July 2013 / Accepted: 13 August 2013 / Published online: 24 August 2013

Abstract Soft (SS) and hard (HS) stearins obtained from high-oleic high-stearic sunflower oil were isothermally crystallized under dynamic (with agitation) and static conditions at 16, 17, 18, 19, and 20 °C and 24, 25, 26, 27, and 28 °C, respectively. Both fractions crystallized under the α-form at early stages of crystallization for all temperatures (T_c) tested. Polymorphic behavior strongly changed with T_c and shear conditions for both fractions. SS fractions were characterized by α, β_2 and/or β_1 polymorphs at lower T_c and β_1 crystals at higher T_c when crystallized under dynamic conditions, while this same fat system was characterized by β_2' crystals at lower T_c and β_2 at higher T_c under static conditions. HS samples were mainly characterized by α and β_2 crystals at lower T_c and α and β_1 crystals at higher T_c when crystallized under dynamic conditions; while the same fat was characterized by β_1' crystals when crystallized at lower T_c and α when crystallized at higher T_c under static conditions after 90 min at T_c. These different polymorphic behaviors, in combination with the different processing and tempering temperatures are translated in specific textural behavior of the samples.

Keywords Polymorphism · Fats · High stearic high oleic sunflower oil · Crystallization · Texture · Morphology · Thermal behavior

S. Martini (✉) · Y. Ye · C. Y. Tan
Department of Nutrition, Dietetics, and Food Sciences, Utah State University, 8700 Old Main Hill, Logan, UT 84322-8700, USA
e-mail: silvana.martini@usu.edu

J. A. R. Cardona · R. J. Candal
School of Science and Technology, UNSAM, Campus Miguelete, San Martín, Buenos Aires Province, Argentina

R. J. Candal
CONICET, INQUIMAE, University of Buenos Aires, 1428 Ciudad Universitaria, Buenos Aires, Argentina

M. L. Herrera
Facultad de Ciencias Exactas y Naturales (FCEN), Universidad de Buenos Aires (UBA), Ciudad Universitaria, Buenos Aires, Argentina

Introduction

Fractionation is a common technique used in edible fats and oils to separate triacylglycerols of different melting points. The main objective of this processing technique is to obtain lipid fractions with different melting points, and therefore different physicochemical properties and functionalities. Fractionation can be accomplished using different methods: (a) dry fractionation, (b) solvent fractionation, and (c) aqueous detergent fractionation [1]. In general, when an oil is fractionated, a liquid fraction (olein) and a solid-like fraction (stearin) are obtained. High-oleic high-stearic sunflower oil (HOHSSFO) is a new variety of sunflower oil that is characterized by high amounts of stearic acid. This particular characteristic makes it an ideal oil to use in fractionation. Bootello et al. [2, 3] studied the crystallization behavior of HOHSSFO and used dry and solvent fractionation techniques to obtain soft and a hard stearins, respectively. These novel stearins have the potential for being used as cocoa butter equivalents and in the manufacture of shortenings [4]. The quality of lipid-based foods strongly depends on the physicochemical properties of the lipids used in their formulations, which in turn are a consequence of the crystallization behavior of the system. Therefore, understanding the crystallization behavior of the HOHSSFO fractions and quantifying their physicochemical properties, such as

crystal morphology, polymorphism, melting behavior, solid fat content (SFC), and texture, are important to broaden the uses of these fractions in the food industry. The crystallization behavior of lipids strongly depends on the processing conditions used including crystallization temperature, agitation, and cooling rate among others [5–10].

The objective of this paper is to study the isothermal crystallization of HOHSSFO stearins under dynamic and static conditions to evaluate the effect of shear on the physical properties of the crystalline network obtained. The crystallization behavior of the systems was followed by polarized light microscopy (PLM) and the physical characteristics of the crystal network obtained were evaluated using differential scanning calorimetry (DSC), pulse nuclear magnetic resonance (p-NMR), texture analysis. Wide (WAXS) and small (SAXS) angle X-ray scattering with a synchrotron source was used to identify the polymorphic form associated with specific crystal morphologies.

Materials and Methods

Starting Material

Two commercial HOHSSFO stearins from Mar del Plata, Buenos Aires, Argentina were used in this study. Stearins were obtained as described by Salas et al. [3] and Rincón-Cardona et al. [11]. In short, a soft stearin (SS) was obtained through dry fractions of the HOHSSFO while a hard stearin (HS) was obtained using a solvent fractionation of the oil. The fatty acid methyl ester and triacylglycerol composition of these samples was reported by Rincón-Cardona et al. [11].

Melting Point Determination

The melting point of HOHSSFO stearins was determined using AOCS Method Cc 1-25 [12].

Dynamic Crystallization

Samples were placed in a double-walled 150-ml beaker (7 cm e.d. × 5 cm i.d. × 10 cm tall) that allowed for temperature control using an external water bath. A schematic representation of the beaker can be found in Martini et al. [13]. Samples were melted in the beaker at 60 °C and kept at this temperature for 30 min and then cooled to the T_c at 1 °C/min using 200 rpm of agitation using a magnetic stirrer (3.7 cm long × 0.7 cm diameter). SS were crystallized at 16, 17, 18, 19, and 20 °C while HS were crystallized at 24, 25, 26, 27, and 28 °C. Samples were kept at T_c for 90 min, where time zero corresponds to the moment when samples reached T_c. The morphology of the crystals obtained and the SFC of the system was measured as a function of crystallization time as described below. After 90 min at T_c, the melting behavior of the crystalline network formed was evaluated using DSC. At this point, samples were placed in 1-cm diameter tubes and stored at T_c for 48 h to measure the texture and the melting behavior of the crystalline network formed.

Static Crystallization

Samples were melted at 60 °C in an oven and kept at this temperature for at least 30 min. Then, samples were placed in appropriate sample holders (1-cm diameter plastic tubes for texture, NMR tubes for SFC determination, DSC pans, or slides for PLM) and cooled to T_c at 1 °C/min. SS were crystallized at 16, 17, 18, 19, and 20 °C while HS were crystallized at 24, 25, 26, 27, and 28 °C. The morphology of the crystals formed and the SFC of the samples were measured as a function of crystallization time, where time zero corresponds to the moment when the sample reaches the crystallization temperature. Samples were stored for 48 h at T_c and the melting profile and texture was measured at this point. These different techniques are commonly used in lipid crystallization research and no significant differences in the crystallization behavior of the materials as a consequence of the slightly different geometries are expected.

Microstructure of Crystals

The morphology of the crystals obtained during dynamic crystallization was evaluated using a polarized light microscope (Olympus BX 41, Olympus America Inc., Melville, NY, USA) equipped with a digital camera (Lumenera Infinity 2). During static crystallization, crystals were observed with a polarized-light microscope Axio Scope.A1 (Carl Zeiss, Goettingen, Germany) equipped with a video camera AxioCam ERc 5 s, with temperature control through a thermal stage Instec's TS62 connected to a computer. Axio Vision 4 software was used to collect the images.

Solid Fat Content (SFC)

The SFC of samples crystallized under dynamic conditions was measured using p-NMR (NMS 120 Minispec NMR Analyzer, Bruker, Rheinstetten, Germany) while the SFC of samples crystallized under static conditions was measured by with a Bruker mq 20 minispec analyzer (Bruker, Rheinstetten, Germany) using a cell with temperature control. The crystallization process of all samples was studied by measuring SFC as a function of time for a total

of 90 min. Since these are isothermal experiments, time zero corresponds to the time when the samples reach T_c. For the dynamic crystallization, an aliquot of the crystallizing material was taken from the beaker, placed in the NMR tube and measured for SFC. For the static measurements molten samples were placed in NMR tubes and cooled at 1 °C/min to reach T_c (T_c = 16, 17, 18, 19 and 20 °C for SS and 24, 25, and 26 °C for HS). Samples were measured in triplicate and results are expressed as averages and standard deviations.

Texture

Hardness was measured in the samples crystallized under dynamic and static conditions. When samples were crystallized under dynamic conditions, samples were placed in a 1-cm diameter plastic tube after 90 min of dynamic crystallization, placed in a water bath equilibrated at T_c, and kept at T_c for 48 h. For the samples crystallized under static conditions, melted samples were placed in plastic tubes of 1 cm diameter, cooled at 1 °C/min to reach T_c and left at T_c for 48 h using a water bath. After 48 h, samples were taken out of the tubes and 1-cm tall cylinders were cut and placed in the texture analyzer. SS were crystallized at 16, 17, 18, 19, and 20 °C, while HS were crystallized at 24, 25, 26, 27 and 28 °C. A TMS-Pro texture analyzer was used (Texture Technologies Corp., Scarsdale, NY/Stable Micro Systems, Godalming, Surrey, UK) using a 500 N probe. Samples were measured at room temperature with a flat cylindrical geometry. The force required to reach 25 % compression was recorded as a function of time.

Melting Behavior

Melting behavior of the samples crystallized under static and dynamic conditions was measured using a differential scanning calorimeter (DSC-TA Instruments Q20). The melting behavior of samples after 90 min and after 48 h at T_c was measured. Samples were placed in hermetically sealed aluminum pans and heated from T_c to 60 °C at 5 °C/min. The melting behavior was quantified with the onset melting temperature (T_{on}), peak melting temperature (T_p), and melting enthalpy (ΔH).

X-Ray Studies

X-ray diffraction measurements were performed to identify specific polymorphic forms associated with different crystal morphologies in SS and HS samples. Since the same types of crystals were observed in SS and HS samples these experiments were only performed for HS samples under static conditions. The polymorphic forms were measured using a synchrotron X-ray scattering equipment (small and wide angle, SAXS and WAXS, respectively) at the SAXS1 beamline of the Synchrotron National Laboratory (LNLS, Campinas, Brazil) with a 1.55 Å wavelength. The scattering intensity distributions as a function of scattering angle (2θ) were obtained in the 2θ range between 0.88° and 27.68°. 15 mg of sample was placed in a hermetical aluminum pan with a transparent circle of 4 mm of diameter in both base and lid and exposed to X-ray beam. Sample were melted to 60 °C at 10 °C/min, then they were kept isothermally at 60 °C for 15 min to erase any crystal memory, and finally they were cooled to crystallization temperature at 1 °C/min. Zero time was the moment at which samples reached crystallization temperature. HS samples were crystallized at 23, 24, 25 and 26 °C to obtain the different crystal morphologies. X-ray diffraction experiments were only performed for HS stearins since the objective is to match specific crystal morphology with polymorphic behavior. A more detailed study of the polymorphic behavior of these systems (SS and HS) was previously reported [11].

Results and Discussion

Characteristics of Starting Materials

SS and HS samples had melting points of 30.6 ± 0.1 and 35.7 ± 0.1 °C, respectively. The main fatty acids present in these samples were stearic (18:0) and oleic acids (18:1). Stearic acid content was 28.1 ± 0.5 and 46.9 ± 0.7 % for the SS and HS, respectively; while oleic content for SS and HS was 58.8 ± 0.2 and 39.9 ± 0.3 %, respectively.

Crystal Morphology and Polymorphism

The objective of these experiments was to characterize all the possible morphologies observed in SS and HS samples in terms of their polymorphism. To achieve this complete characterization of crystalline morphology, specific T_c and crystallization times were chosen to obtain specific crystal morphologies and polymorphic forms. During dynamic and static crystallization conditions, SS and HS samples were characterized by five different morphologies (see details in the next section). Each morphology type corresponds to a different polymorphic form as described by Rincón-Cardona et al. [11]. The relationship between crystal morphology and polymorphism is summarized here with a series of experiments performed with HS samples crystallized at 23, 24, 25 and 26 °C for different periods of time. The first type of crystal morphology that we will describe is characterized by small needle-like crystals which correspond to an α polymorph with a strong peak at 0.42 nm (Fig. 1a). This type of morphology was obtained when HS

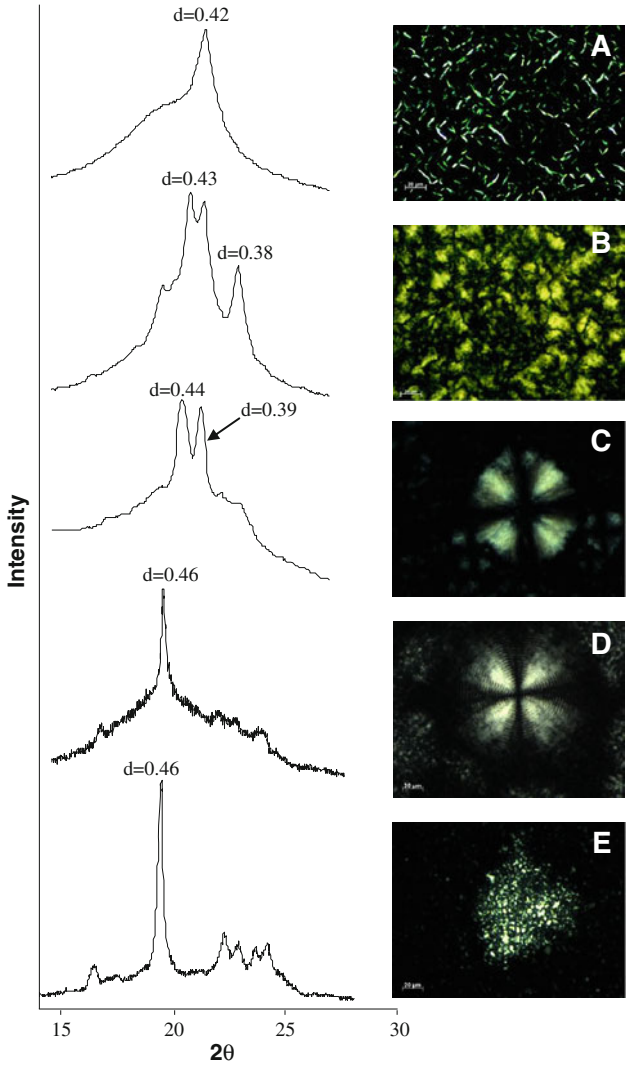

Fig. 1 WAXS patterns and morphology by PLM of α, β_2', β_1', β_2, and β_1 forms of HS crystallized under static conditions. **a** 10 min at 23 °C **b** 20 min at 23 °C **c** 60 min at 24 °C **d** 6 h at 25 °C **e** 48 h at 26 °C

sample was crystallized at 23 °C for 10 min. After 20 min at this same T_c, α crystals changed from needle-like to ill-defined spherulites that correspond to a β_2' polymorphic form characterized by two signals in the WAXS: one at 0.43 and one at 0.38 nm (Fig. 1b). The third type of crystal morphology observed was a well-defined spherulite with distinctive Maltese crosses shapes which corresponded to β_1' polymorphism characterized by two signals in the WAXS at 0.44 and 0.39 nm (Fig. 1c). In this particular situation, β_1' polymorphism was obtained after 60 min at 24 °C. The forth type of morphology observed in these samples was also a well-defined spherulite similar to the spherulites obtained for β_1' polymorphism, but in this case, the spherulites had very distinctive concentric lines or patterns that were not observed in the β_1' crystals. These morphologies corresponded to β_2 crystals characterized by one strong signal at 0.46 nm (Fig. 1d). The last morphology observed was of an ill-defined agglomeration of crystals with no apparent organization. These crystals corresponded to a β_1 polymorph characterized by a strong signal at 0.46 nm (Fig. 1e). Even though β_2 and β_1 polymorphisms have the same signals in the WAXS spectra, their SAXS spectra is significantly different with signals at 6.06 and 3.02 nm for the β_2 polymorphism and 6.49 and 3.71 nm for the β_1 polymorphic form. A detailed characterization of the polymorphic forms of HS and SS samples can be found in Rincón-Cardona et al. [11]. The identification of these different morphologies to specific polymorphic forms will facilitate the discussion presented in the next sections of this research.

Morphology of Crystals Obtained During Dynamic Crystallization

Figure 2 shows PLM pictures of crystals obtained during dynamic crystallization of SS samples at different crystallization temperatures as described in the "Materials and Methods" section. Small and several crystals were observed at initial times of crystallization, especially for samples crystallized between 17 and 20 °C. Even though samples crystallized at 16 °C showed an evident turbidity at 15 min, crystals were hard to detect in the PLM since they immediately melted on the slide. According to X-ray studies (Fig. 1a) these small crystals correspond to the α polymorph as described by Rincón-Cardona et al. [11]. It is evident from Fig. 2 that the morphology of the crystals significantly changed as crystallization progressed. Typical β_2 spherulites were observed at 30 min when samples were crystallized at 16 °C. The appearance of β_2 spherulites was delayed as T_c increased and no β_2 crystals were obtained for SS samples crystallized at 20 °C. In addition to the presence of α and β_2 crystals, a third morphology can be observed in SS samples crystallized at 16 °C for 60 and 75 min and at 20 °C for 75 and 90 min which is due to the presence of β_1 polymorph.

Figure 3 shows the morphology of crystals obtained when HS samples were crystallized at 24, 25, 26, 27, and 28 °C under dynamic conditions. Similar to the results previously described for SS samples, α crystals were observed at early stages of the crystallization process with the formation of β_2 crystals at 60 and 75 min for samples crystallized at 24 and 25 °C, respectively. β_2 forms then transitioned to β_1 at 90 min for samples crystallized at 24 and 25 °C. For T_c above 25 °C, HS crystallized in a β_1 polymorph as observed, for example, for HS sample crystallized at 26 °C for 60 min. It is interesting to note that when SS and HS samples were crystallized under dynamic conditions, no β_2' or β_1' was observed and a $\alpha \rightarrow \beta_2$ or β_1 transition was observed.

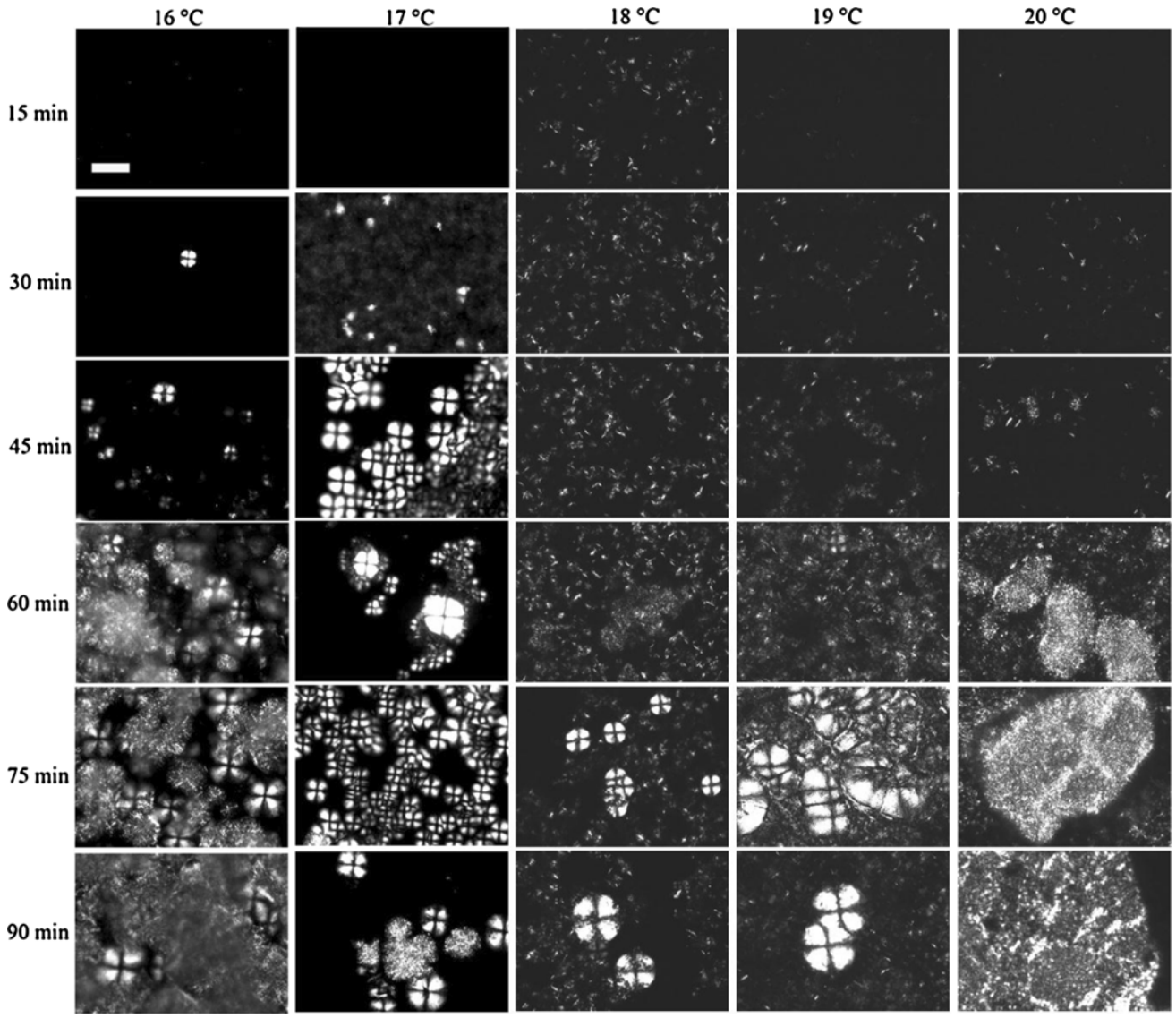

Fig. 2 PLM pictures of crystals obtained for the HOHSSFO soft stearin (SS) crystallized under dynamic conditions as a function of time and crystallization temperature. Zero time corresponds to the moment when the sample reaches crystallization temperature. *White bar* 100 μm

Morphology of Crystals Obtained During Static Crystallization

Figures 4 and 5 show the morphology of crystals obtained when SS and HS samples were crystallized under static conditions under the polarized light microscope. As expected, small α crystals were obtained for SS samples crystallized at 16 and 17 °C (Fig. 4) which transformed into β_2' after 45 min at T_c. The $\alpha \rightarrow \beta_2'$ transformation was delayed at higher temperatures, with β_2 crystals seen for the first time after 60 min for SS samples crystallized at 18 °C. When SS samples were crystallized at $T_c \geq 18$ °C β_2 crystals are mainly observed. The morphology of crystals obtained under static conditions is significantly different from the ones obtained under dynamic conditions. As previously discussed and shown in Fig. 2, β_2 and β_1 crystals are observed at low T_c when SS samples are crystallized under dynamic conditions, while β_2 polymorphic forms are only observed at higher temperatures under static conditions. In addition, β_2' crystals are observed under static conditions while they are not obtained under dynamic ones.

When HS samples were crystallized under static conditions a $\alpha \rightarrow \beta_1'$ transformation was observed at 30 min for $T_c = 24$ °C (Fig. 5). This transformation was delayed at 25 °C and was not observed at 26 and 27 °C. No crystals were observed for HS sample crystallized at $T_c = 28$ °C even after 90 min. It is interesting to note that no β crystals are formed under static conditions for HS samples for the T_c tested in this research. Comparison of dynamic and

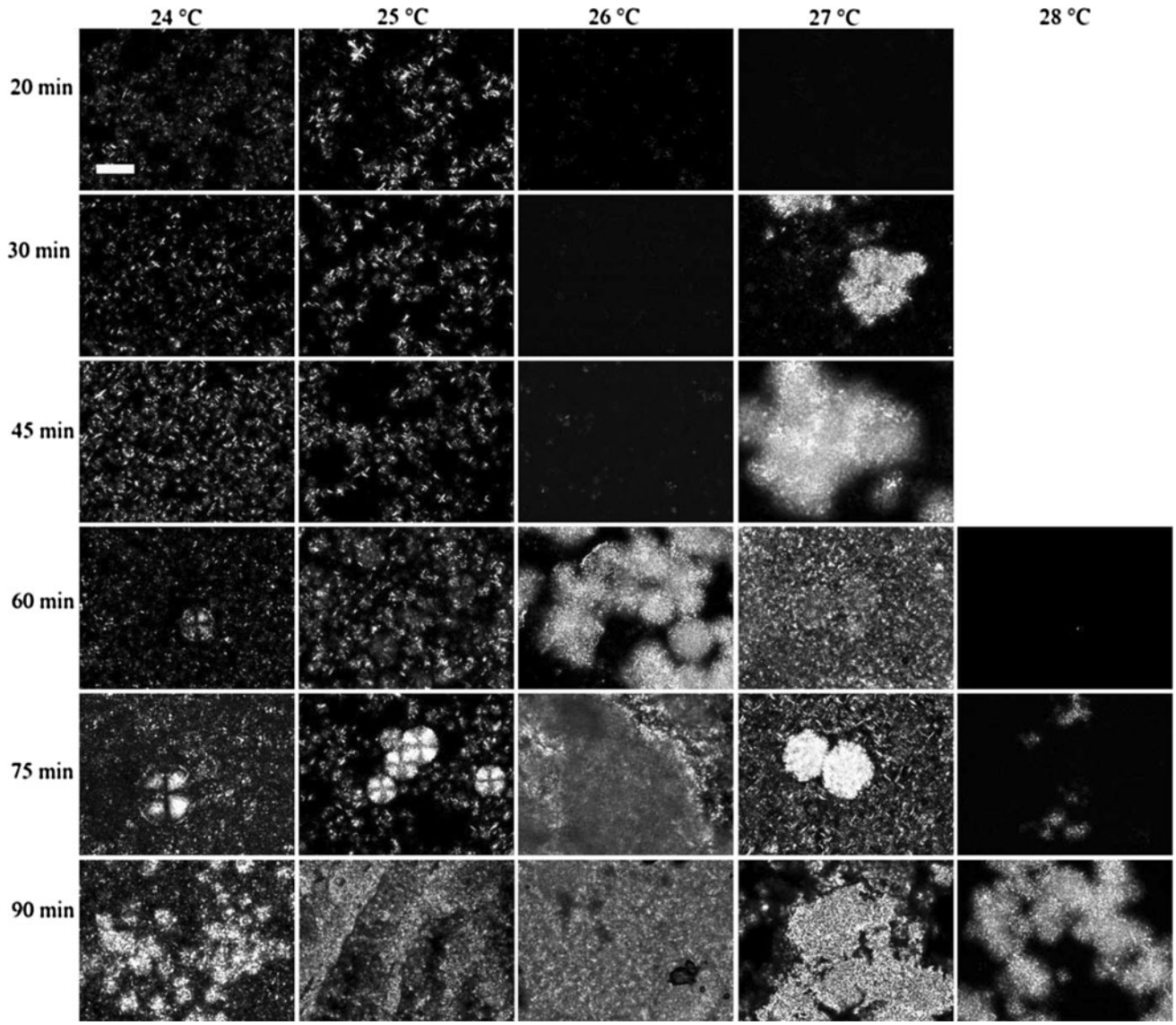

Fig. 3 PLM pictures of crystals obtained for the HOHSSFO hard stearin (HS) crystallized under dynamic conditions as a function of time and crystallization temperature. Zero time corresponds to the moment when the sample reaches crystallization temperature. *White bar* 100 μm

static micrographs of HS samples suggest that static conditions promote $\alpha \rightarrow \beta_1'$ transition and delay the formation of β crystals. In addition, crystallization under static conditions is delayed as evidenced by a lack of crystals for the HS sample crystallized at 28 °C under static conditions.

Solid Fat Content (SFC) Obtained Under Dynamic and Static Conditions

Figure 6 shows the SFC of SS and HS samples crystallized at the T_c mentioned in the "Materials and Methods" section under dynamic and static conditions. As expected, SFC increased as a function of time for samples crystallized under dynamic and static conditions. Interestingly, T_c did not affect the final SFC of SS and HS samples crystallized under dynamic conditions with values of 28.4 ± 0.9, 25.9 ± 0.9, 25.2 ± 0.2, 23.0 ± 2.0, and 22.3 ± 2.4 % for SS crystallized for 90 min at 16, 17, 18, 19, and 20 °C, respectively and 39.2 ± 1.8, 32.0 ± 4.7, 28.1 ± 6.0, 17.2 ± 0.1, and 15.1 ± 5.6 % for HS crystallized for 90 min at 24, 25, 26, 27, and 28 °C, respectively. However a tendency of lower SFC values was observed as T_c increased. In addition, SFC values obtained for HS were in general higher than the ones obtained for SS samples, especially at lower T_c. The SFC of SS and HS samples crystallized under static conditions was affected by time and T_c. Higher T_c resulted in lower SFC values with SFC of approximately zero for $T_c \geq 19$ °C for SS samples and $T_c \geq 25$ °C for HS samples. As previously mentioned, a significant delay in the crystallization of SS

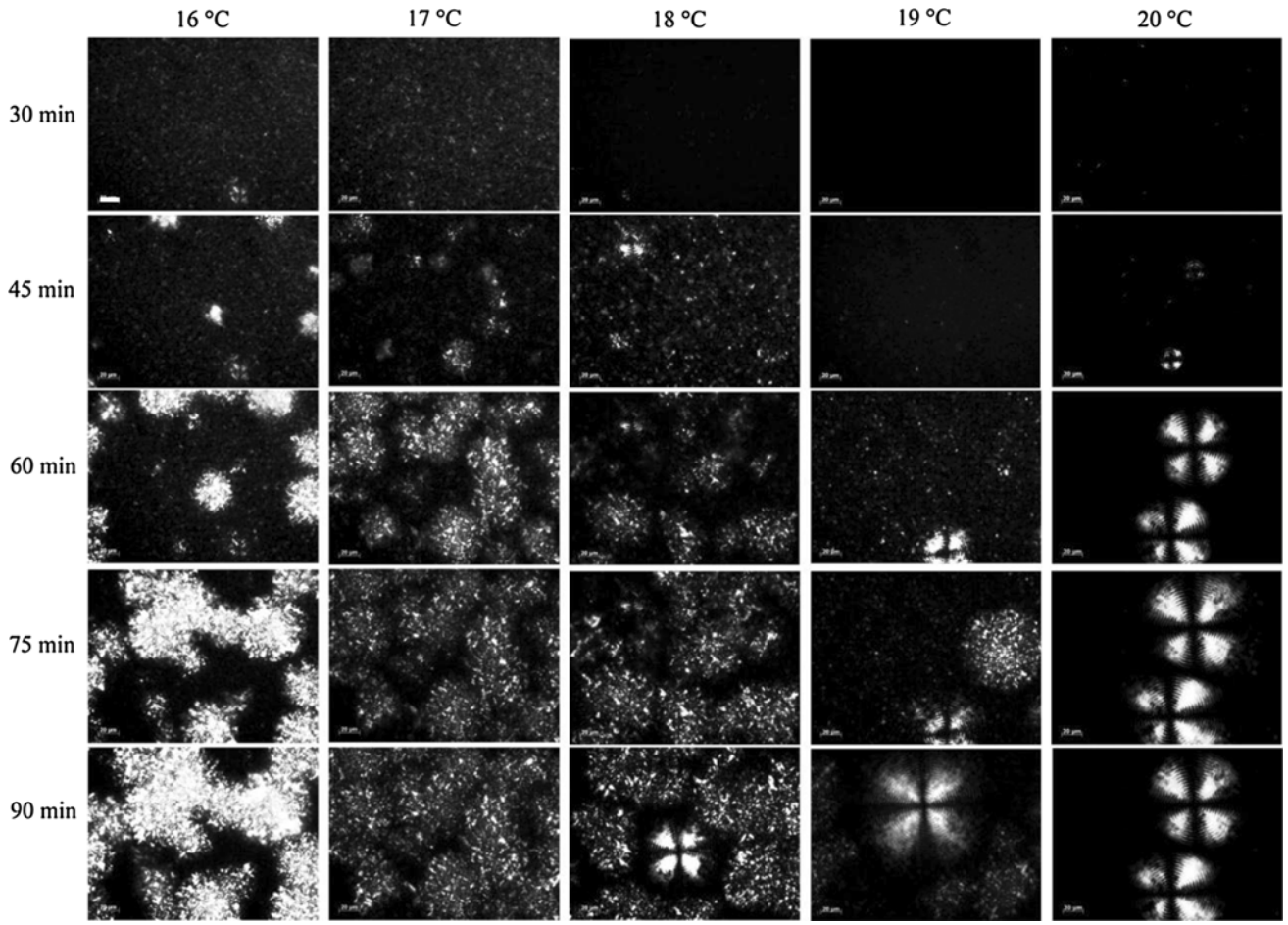

Fig. 4 PLM pictures of crystals obtained under static conditions for SS samples as a function of time and crystallization temperature. Zero time corresponds to the moment when the sample reaches crystallization temperature. *White bar* 20 μm

and HS samples is observed when crystallized under static conditions. However, for certain T_c, the SFC obtained after 90 min of crystallization was higher for samples crystallized under static conditions. For example, the SFC of SS samples after 90 min at T_c under static conditions was 32.3 ± 0.3 and 27.0 ± 1.7 % for samples crystallized at 16 and 17 °C, respectively. Similarly, the SFC of HS samples crystallized for 90 min at 24 °C under static conditions was 60.9 ± 1.1 %. These results suggest that crystallization under static conditions delays the nucleation of crystals but promotes crystal growth.

Melting Behavior of Samples Crystallized Under Dynamic and Static Conditions

Figure 7 shows the melting profiles of SS and HS samples after 90 min of isothermal crystallization at the T_c under dynamic and static conditions. Broad melting profiles can be observed in SS and HS samples at all the T_c tested. These broad melting profiles with the presence of shoulders suggest that different polymorphic forms co-exist in the samples' tested. This behavior seems to be very evident for SS samples crystallized at 16, 17, and 18 °C and even more evident for samples crystallized under static conditions. The co-existence of different polymorphic forms for SS crystallized under dynamic conditions can be corroborated through the PLM images where α, β_2 and β_1 crystals co-exist at these temperatures (Fig. 2). When SS samples are crystallized under static conditions a very broad peak with significant fractionation was observed when the sample is crystallized at 18 °C. Figure 4 shows that under this condition, α, β_2' and β_2 crystals co-exist and these different polymorphic forms might be responsible for the fractionation observed in the melting profiles. The DSC melting profiles also show a significant delay in the crystallization of samples crystallized under static conditions where significantly smaller peaks are observed for SS samples crystallized at 19 and 20 °C and no peaks are observed for HS samples crystallized at 26–28 °C. Tables 1 and 2 show the onset (T_{on}) and peak (T_p) melting temperatures together with the melting enthalpies (ΔH) for SS and HS samples crystallized under dynamic and static conditions. No

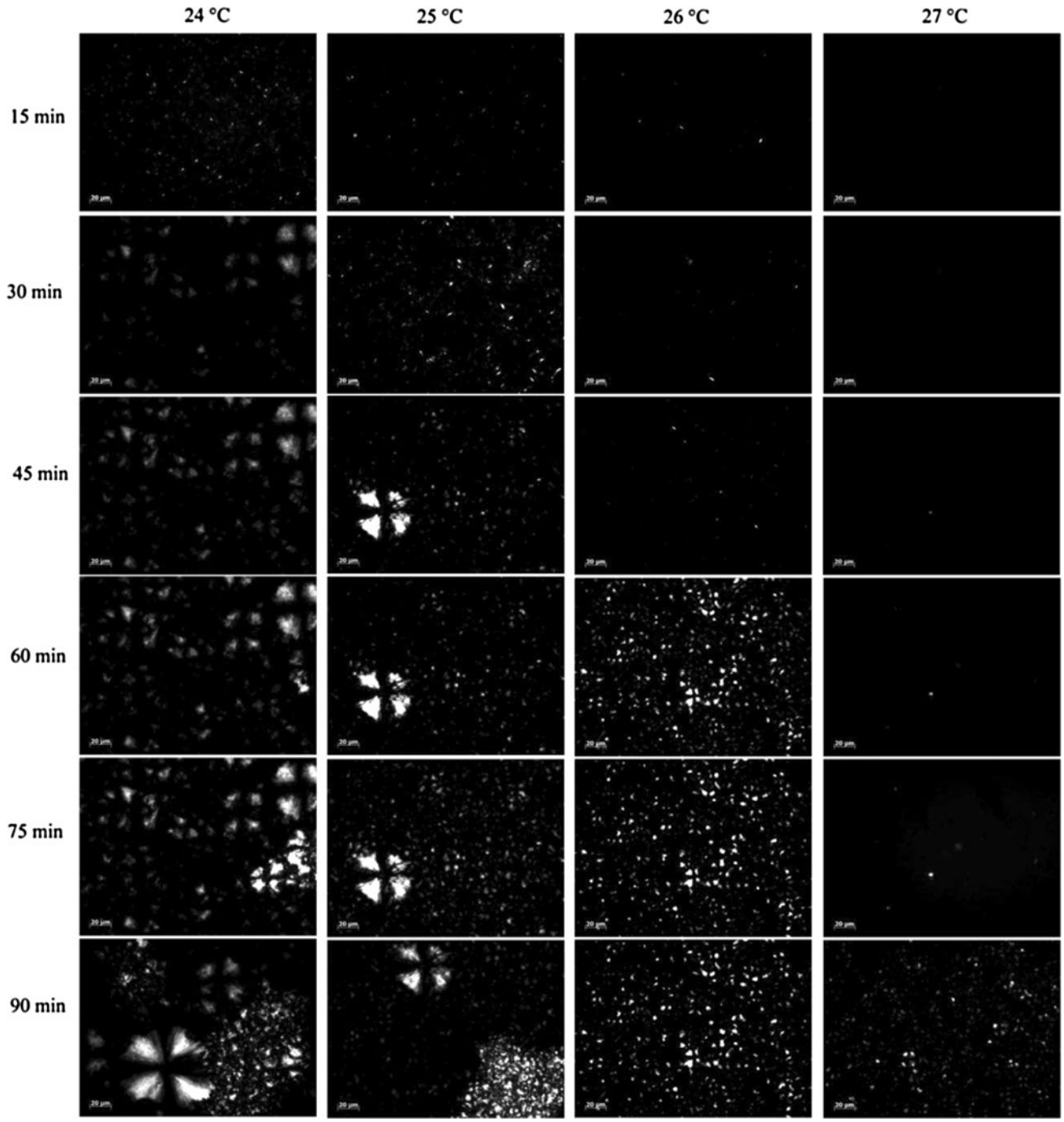

Fig. 5 PLM pictures of crystals obtained under static conditions for HS samples as a function of time and crystallization temperature. Zero time corresponds to the moment when the sample reaches crystallization temperature. *White bar* 20 μm

significant differences ($\alpha = 0.05$) were found in the enthalpy values of SS samples crystallized at different T_c and under dynamic and static conditions with a mean value $\Delta H = 34.6 \pm 5.6$ J/g. Significant differences ($p < 0.05$) were found for the T_{on} and T_p values for SS samples. In general, T_p values were lower for SS samples crystallized under static conditions and T_p values decreased at higher T_c. T_{on} were also affected by T_c and crystallization conditions. T_{on} values were significantly lower for samples crystallized at 17 and 18 °C in SS samples crystallized under dynamic conditions and at 18 °C when SS samples were crystallized under static conditions. This means that at these T_c broader melting profiles are observed as described in Fig. 7. This broader profile might be a consequence of the co-crystallization of different molecular species and/or the formation of difference polymorphic

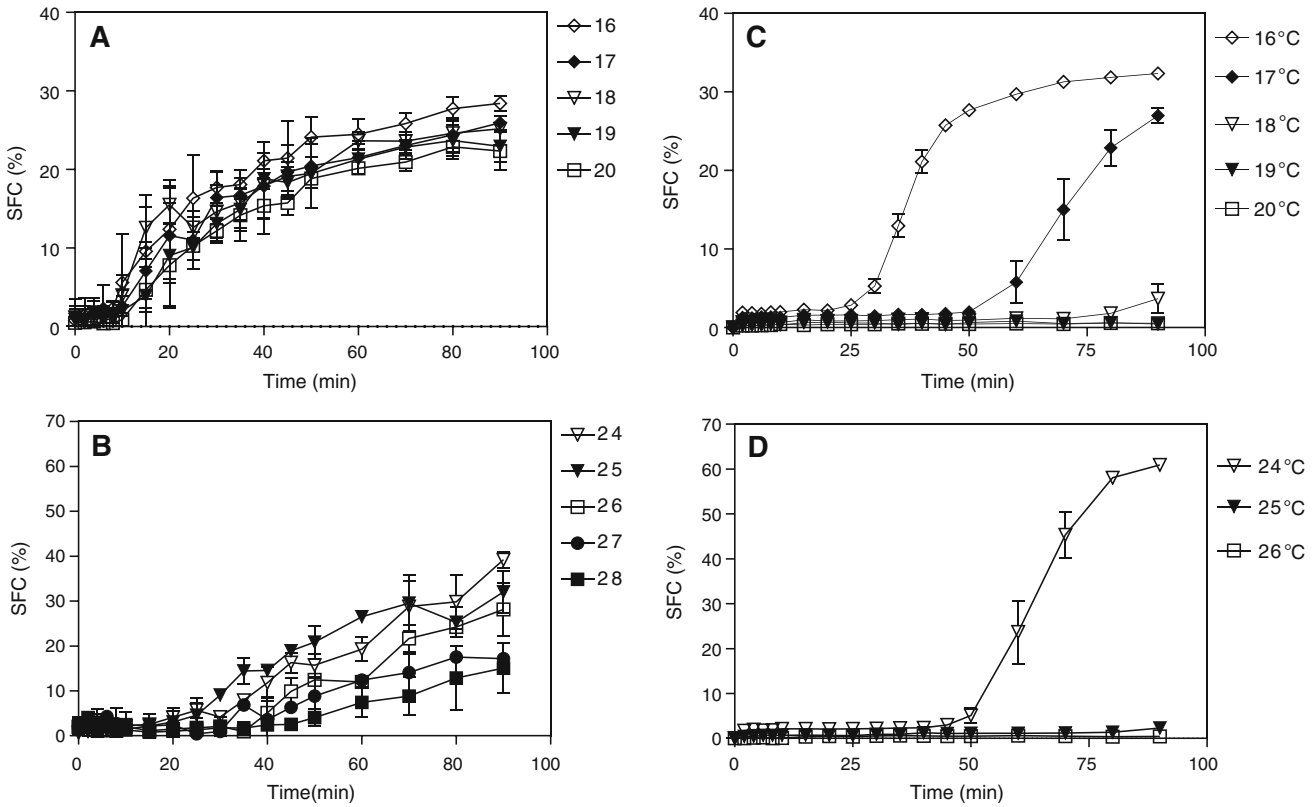

Fig. 6 SFC of SS (**a**, **c**) and HS (**b**, **d**) samples crystallized under dynamic (**a**, **b**) and static (**c**, **d**) conditions at different crystallization temperatures. SFC data are expressed as mean values and standard deviations of three replicates

forms. Significant differences were found for T_{on}, T_p, and enthalpy values among HS samples crystallized at different T_c under dynamic and static conditions (Table 2). T_c did not affect these values in a great extent while the biggest differences were observed between the values obtained under dynamic and static conditions with mean values of $T_{on} = 33.3 \pm 1.0$ °C, $T_p = 38.3 \pm 1.4$ °C, and $\Delta H = 104.9 \pm 10.2$ J/g for the dynamic conditions and $T_{on} = 27.3 \pm 0.1$ °C, $T_p = 31.1 \pm 0.1$ °C, and $\Delta H = 35.9 \pm 4.6$ J/g for the static conditions. The significantly lower values of enthalpy observed for the HS conditions is an indication of the delay in crystallization observed under static conditions.

Hardness of Samples Crystallized Under Dynamic and Static Conditions

In addition to crystal morphology and polymorphism, hardness is one of the most important physical properties of lipids that must be quantified in food applications. In general, the hardness of lipid samples is measured after tempering the samples for 24 or 48 h to ensure that the most stable crystal structure and organization is achieved. In our experiments, hardness was measured after crystallizing the samples under dynamic and static conditions and tempering for 48 h at T_c. Results are presented in Fig. 8. The texture profiles of SS samples crystallized under dynamic and static conditions are characterized by two peaks. The first peak measures the fracturability or brittleness of the sample, while the second peak measures the hardness of the sample. Fracturability values are usually lower than hardness values. Figure 8a and c show the first and second peak values obtained for SS samples crystallized under dynamic and static conditions, while Fig. 8d and f show the first and second peak values obtained for HS samples crystallized under dynamic and static conditions. SS samples fractured at all T_c tested (Fig. 8a). The texture profile of HS samples only show a fracturability peak for $T_c = 28$ °C (Fig. 8d) which is evidenced by a lower value reported in Fig. 8d at 28 °C compared to the value reported in Fig. 8f. Since no fracturability peak was observed in HS samples crystallized at $T_c < 28$ °C the peak values reported in Fig. 8d are the same as the ones reported in Fig. 8e for these T_c. The maximum fracturability value for SS was obtained for samples crystallized at 17 °C under static conditions and was not significantly different from the fracturability value obtained at 16 °C. As T_c increases, fracturability values slowly decrease. It is interesting to note the similar values of fracturability between the samples crystallized at 16 and 17 °C even though the SFC was significantly higher for samples crystallized at 16 °C.

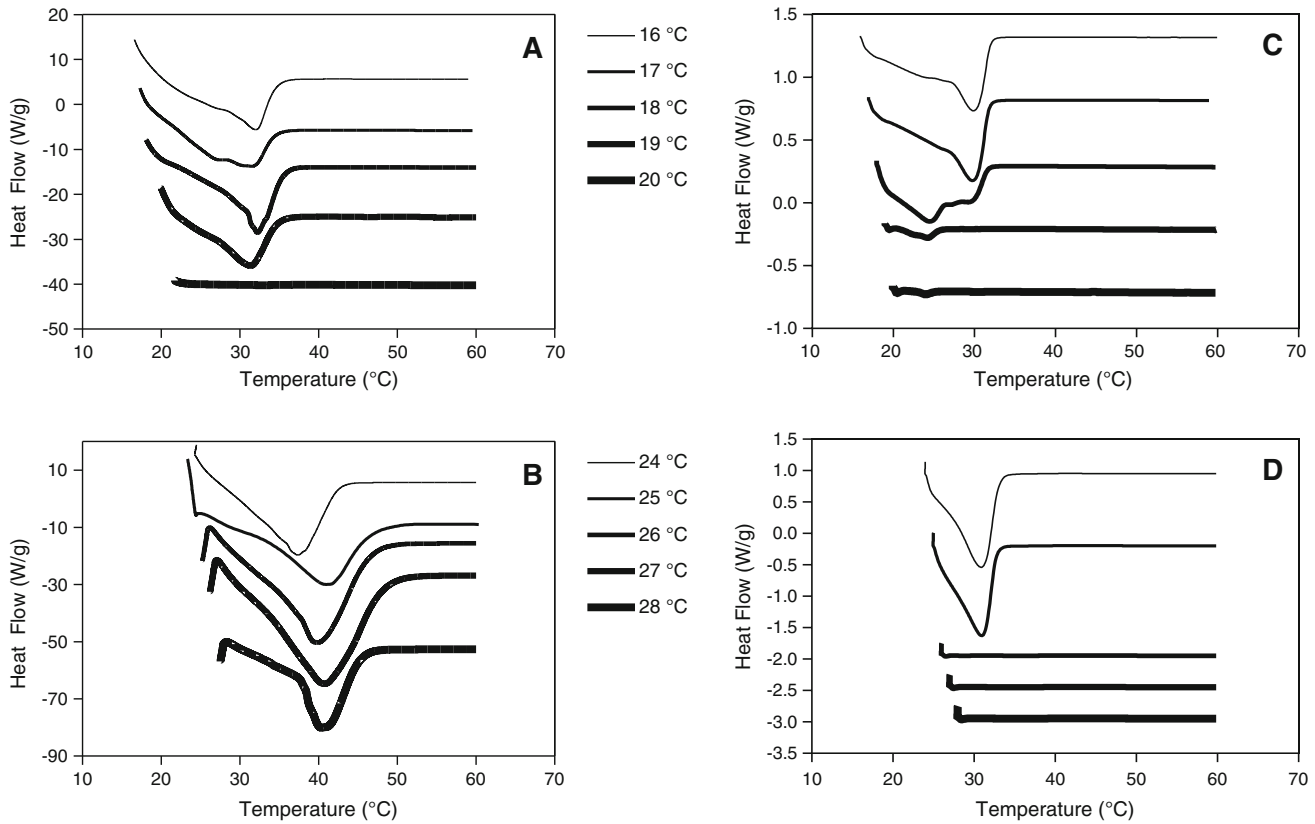

Fig. 7 DSC melting profiles of SS (**a**, **c**) and HS (**b**, **d**) crystallized under dynamics (**a**, **b**) and static (**c**, **d**) conditions for 90 min at different temperatures. Time zero corresponds to the time when sample reaches crystallization temperature

Table 1 Melting parameters obtained using DSC for the SS sample crystallized under dynamic and static conditions after 90 min at T_c

T_c (°C)	T_{on} (°C)	T_p (°C)	Enthalpy (J/g)
Dynamic			
16	27.0 ± 2.9^{a}	32.1 ± 0.1^{a}	36.1 ± 4.9
17	20.9 ± 1.7^{b}	31.4 ± 0.2^{b}	32.4 ± 7.6
18	23.9 ± 0.1^{a}	31.1 ± 0.1^{bd}	43.6 ± 7.4
19	24.8 ± 0.6^{a}	30.6 ± 0.1^{d}	36.8 ± 15.8
20	27.5 ± 2.1^{a}	31.6 ± 0.0^{ab}	38.6 ± 3.8
Static			
16	25.9 ± 0.8^{a}	29.9 ± 0.1^{c}	30.5 ± 5.1
17	25.4 ± 1.1^{a}	29.8 ± 0.2^{c}	34.2 ± 4.0
18	20.6 ± 0.6^{b}	24.3 ± 0.3^{e}	24.9 ± 2.0
19	N/A	N/A	N/A
20	N/A	N/A	N/A

Data reported are mean values and standard deviations for two replicates

Data in the same column with the same superscript are not significantly different ($\alpha = 0.05$)

No significant differences were found in the enthalpy values as a function of T_c and processing condition (dynamic vs. static) ($\alpha = 0.05$)

Table 2 Melting parameters obtained using DSC for the HS sample crystallized under dynamic and static conditions after 90 min at T_c

T_c (°C)	T_{on} (°C)	T_p (°C)	Enthalpy (J/g)
Dynamic			
24	32.1 ± 1.2^{ab}	35.9 ± 2.1^{ab}	87.3 ± 2.0^{a}
25	33.0 ± 1.8^{ab}	39.1 ± 2.6^{a}	113.7 ± 9.5^{a}
26	34.4 ± 1.1^{a}	38.5 ± 2.0^{a}	108.6 ± 18.0^{a}
27	32.8 ± 3.4^{ab}	39.4 ± 1.8^{a}	108.5 ± 18.4^{a}
28	34.1 ± 0.9^{a}	38.4 ± 2.1^{a}	106.1 ± 8.9^{a}
Static			
24	27.2 ± 0.8^{b}	31.2 ± 0.1^{b}	39.1 ± 3.9^{b}
25	27.3 ± 0.3^{b}	31.1 ± 0.2^{b}	32.6 ± 3.4^{b}
26	N/A	N/A	N/A
27	N/A	N/A	N/A
28	N/A	N/A	N/A

Data reported are mean values and standard deviations for two replicates

Data in the same column with the same superscript are not significantly different ($\alpha = 0.05$)

Similarly, the SFC of SS crystallized under static conditions was significantly lower at 18 °C and zero at 19 and 20 °C but similar values of fracturability were observed after tempering. These results suggest that samples continue to crystallize

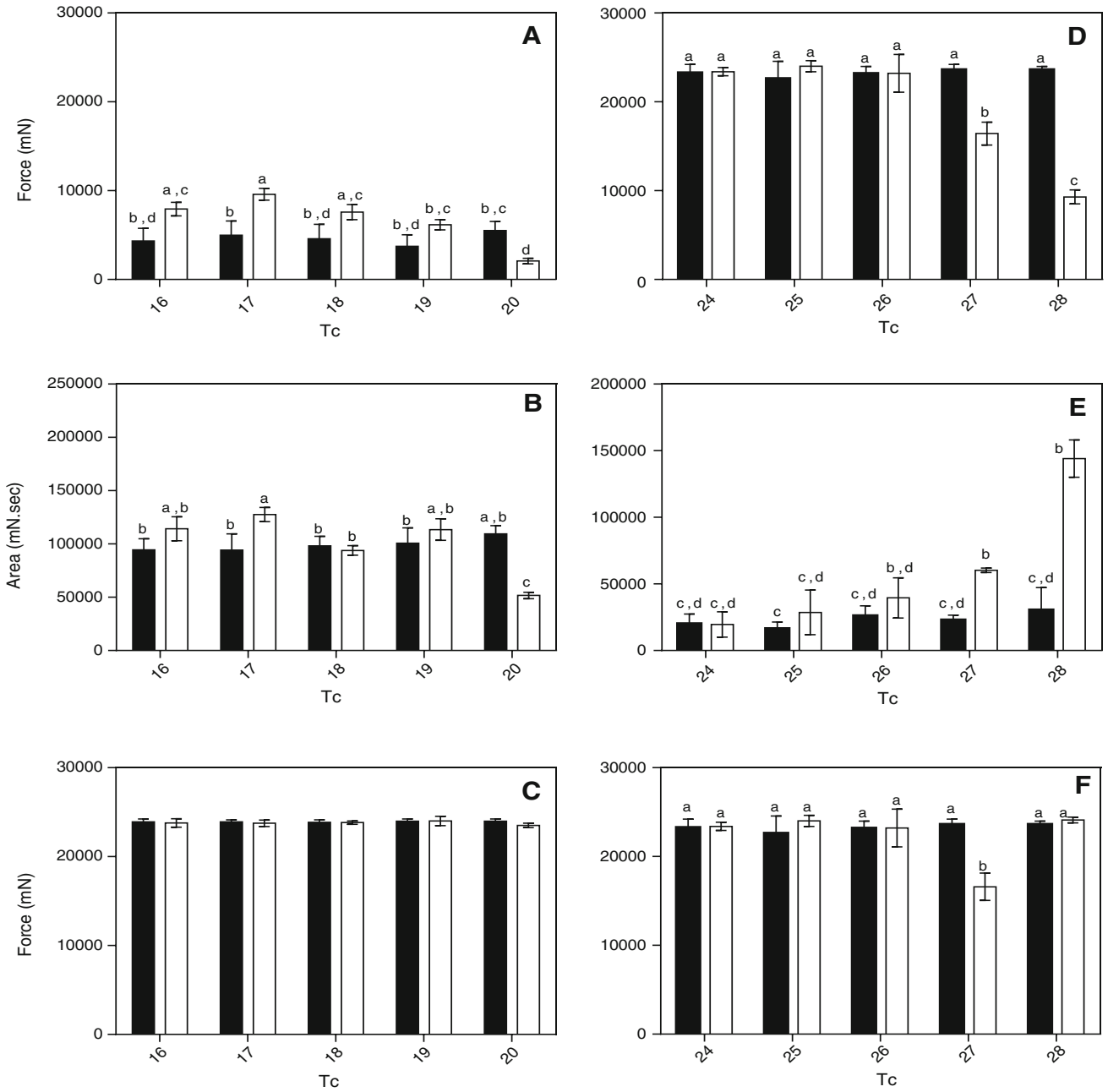

Fig. 8 Texture parameters (*first peak*, *second peak*, and *area*) of SS (**a–c**) and HS (**d–f**) samples crystallized at T_c for 48 h under dynamic (*black bars*) and static (*white bars*) conditions. Data shown are average values of four replicates and standard deviations. In each graphs, *bars* with *the same letters* are not significantly different ($\alpha = 0.05$)

during the tempering process. The further crystallization observed during tempering is also observed in the data presented in Table 3, where the enthalpy values of the tempered SS samples are higher than the ones obtained after 90 min of crystallization (Table 1). The fracturability of SS samples crystallized under dynamic conditions was not significantly ($\alpha = 0.05$) affected by T_c and it was always lower than the fracturability obtained under static conditions, with the exception of samples crystallized at 20 °C. No significant differences were found in the hardness of SS samples crystallized at different T_c under dynamic and static conditions (Fig. 8c). The area under the compression peak was significantly higher ($\alpha = 0.05$) for samples crystallized at 17 °C under static conditions and significantly lower ($\alpha = 0.05$) for samples crystallized at 18 and 20 °C under static conditions. No significant differences were observed in the area under the compression peak for samples crystallized under dynamic conditions. The area under the compression peak is inversely proportional to the gumminess of the sample. It can be seen that the lowest area under the

compression peak was obtained at $T_c = 20$ °C indicating that this sample has the highest gumminess.

As previously mentioned, a fracturability peak was only observed in HS samples crystallized under static conditions at 28 °C. All the other crystallization conditions resulted in a single peak that corresponds to the hardness of the sample. The hardness of HS samples crystallized under dynamic and static conditions and under different T_c was only significant for $T_c = 27$ °C ($\alpha = 0.05$). HS samples crystallized at 27 °C under static conditions were softer. Finally, HS samples crystallized at 28 °C show a fracturability peak which is unusual for this sample. The fracturability of HS samples crystallized under dynamic and static conditions was not significantly different when crystallized at lower T_c (24–26 °C). Similar to the discussion presented for the SS samples, static conditions delayed the crystallization of HS samples and resulted in a higher final SFC at lower T_c. This delay in the crystallization can be also observed in the enthalpy values reported in Table 4, where slightly higher enthalpy values are observed for samples crystallized under dynamic conditions, especially at high T_c (27 and 28 °C). However, after tempering, samples continue to crystallize, especially for the samples crystallized under static conditions (Tables 2, 4). The fact that there is no significant difference in the texture as a function of T_c and processing conditions (dynamic vs. static) suggest that the sample has reached phase equilibrium. It is interesting to note that the area of the compression peak increases exponentially with temperature for samples crystallized under static conditions, suggesting a significant decrease in the gumminess of the sample as T_c increases. No significant differences were observed in the area of the compression peak for samples crystallized under dynamic conditions. In general, the area of the compression peak obtained for samples crystallized under static conditions was higher than the one obtained under dynamic crystallization.

It is interesting to note that the texture parameters were strongly affected by processing conditions: when samples were crystallized under dynamic conditions, no effect on texture parameters were observed in general, while a strong effect of T_c is observed in the texture of samples crystallized under static conditions, especially at higher T_c. It is very likely that the differences observed in the texture of these samples are a consequence of the molecular characteristic of the crystal network formed. That is, polymorphism, crystal size, and melting profile of the samples contribute, in combination, to the final texture of the material. Since all these factors play a simultaneous role in the textural behavior of the samples it is very difficult to identify a single parameter that drives samples' texture. Future research should be performed to evaluate the role of each of these factors on the textural behavior of the samples.

Table 3 Melting parameters obtained using DSC for the SS sample crystallized at different T_c under dynamic and static conditions and tempered for 48 h at T_c

T_c (°C)	T_{on} (°C)	T_p (°C)	Enthalpy (J/g)
Dynamic			
16	30.0 ± 0.6	32.7 ± 0.5^{ac}	48.2 ± 1.8^{ac}
17	30.1 ± 0.4	32.2 ± 0.4^{ab}	41.0 ± 4.0^{b}
18	29.6 ± 1.0	31.8 ± 0.2^{b}	45.2 ± 1.5^{ab}
19	29.3 ± 1.3	32.4 ± 0.2^{abc}	43.6 ± 1.1^{bc}
20	29.1 ± 1.8	32.3 ± 0.0^{abc}	39.7 ± 0.6^{b}
Static			
16	29.4 ± 0.1	32.3 ± 0.1^{ab}	49.4 ± 0.9^{ac}
17	29.9 ± 0.2	31.9 ± 0.3^{ab}	49.9 ± 0.2^{a}
18	30.5 ± 0.1	32.5 ± 0.0^{ac}	48.8 ± 0.4^{a}
19	28.5 ± 2.5	33.0 ± 0.1^{ac}	46.0 ± 0.1^{ab}
20	29.8 ± 0.7	33.1 ± 0.1^{c}	47.6 ± 0.2^{ab}

Data reported are mean values and standard deviations for two replicates

Data in the same column with the same superscript are not significantly different ($\alpha = 0.05$)

No significant differences were observed for T_{on} values between T_c and crystallization conditions (dynamic vs. static) ($\alpha = 0.05$)

Table 4 Melting parameters obtained using DSC for the HS sample crystallized at different T_c under dynamic and static conditions and tempered for 48 h at T_c

T_c (°C)	T_{on} (°C)	T_p (°C)	Enthalpy (J/g)
Dynamic			
24	35.8 ± 0.6^{a}	37.7 ± 0.2^{a}	109.9 ± 5.8^{a}
25	35.1 ± 1.9^{a}	38.4 ± 0.2^{a}	110.1 ± 3.6^{a}
26	36.1 ± 0.7^{a}	38.0 ± 0.3^{a}	109.2 ± 6.1^{a}
27	35.9 ± 0.4^{a}	38.3 ± 0.6^{a}	106.6 ± 3.5^{a}
28	36.0 ± 0.2^{a}	37.8 ± 0.2^{a}	104.9 ± 2.8^{a}
Static			
24	35.0 ± 0.9^{ac}	37.7 ± 0.4^{a}	102.2 ± 2.5^{a}
25	35.4 ± 0.1^{ac}	37.3 ± 0.0^{a}	107.4 ± 1.8^{a}
26	35.3 ± 0.1^{ac}	38.4 ± 0.5^{a}	104.2 ± 3.1^{a}
27	32.2 ± 0.6^{bc}	35.2 ± 0.7^{b}	68.9 ± 2.0^{b}
28	31.7 ± 1.2^{b}	35.4 ± 0.2^{b}	70.4 ± 2.3^{b}

Data reported are mean values and standard deviations for two replicates

Data in the same column with the same superscript are not significantly different ($\alpha = 0.05$)

Melting Behavior of SS and HS Samples Crystallized Under Dynamic and Static Conditions After Tempering for 48 h

After tempering the samples for 48 h at different T_c and measuring their hardness, the melting profile was evaluated using a DSC. Melting parameters are presented in Tables 3

and 4 for the SS and HS samples, respectively. No significant differences ($\alpha = 0.05$) were observed in the T_{on} values ($T_{on} = 29.6 \pm 0.6$ °C) for SS samples crystallized at different T_c using dynamic and static conditions. On the other hand, T_p was affected by T_c and crystallization conditions (dynamic vs. static). The lowest T_p value was obtained for SS samples crystallized at 18 °C, when the sample was under dynamic conditions and at 17 °C when the sample was crystallized under static conditions. Similarly, enthalpy values were affected by T_c and crystallization conditions. As expected, enthalpy values decreased as T_c increased. This effect was more significant for samples crystallized under dynamic conditions. No significant differences ($\alpha = 0.05$) were found for T_{on}, T_p, and enthalpy values among different T_c for HS samples crystallized under dynamic conditions with values of $T_{on} = 35.8 \pm 0.4$ °C, $T_p = 38.0 \pm 0.3$ °C, and $\Delta H = 108.1 \pm 2.3$ J/g. T_{on}, T_p and enthalpy values for samples crystallized under static conditions at low temperatures ($T_c = 24$, 25, and 26 °C) were not significantly different from the ones obtained under dynamic conditions. However, significantly lower values were obtained under static conditions for samples crystallized at higher temperatures ($T_c = 27$ and 28 °C).

It is not surprising to observe significant differences in the polymorphic behavior, crystal morphology, SFC, melting behavior and texture of lipid networks formed under dynamic and static conditions. The effect of agitation on lipid crystallization was previously studied by several authors in different systems. Herrera and Hartel [8–10] showed a slight decrease in the induction of crystallization of milk fat when agitation changed from 50 to 300 rpm. In addition, these authors showed lower storage moduli when samples were crystallized at higher agitation rates and smaller crystals. An increase in the shear modulus with lower agitation was also observed by Kaufmann et al. [14]. Chaleepa et al. [15] also showed an induction in crystallization when coconut oil was crystallized at higher agitation rates evidenced by an increase in SFC. Similar results were described by Narine and Humphrey [16] who showed a strong effect of agitation on the polymorphism, microstructure, and hardness of fully hydrogenated fats such as canola cottonseed, palm, lard, soybean and tallow, blended with soybean oil.

Conclusions

SS and HS fractions obtained from HOHSSFO show very different crystallization behavior. Crystallization temperature and shear strongly affect the crystallization of these systems. Both fractions are polymorphic in nature which translates into different crystal morphologies and textures. Polymorphic behavior strongly changes with T_c for both fractions. SS fractions are characterized by α, β_2 and/or β_1 polymorphs at lower T_c and β_1 crystals at higher T_c when crystallized under dynamic conditions (shear), while this same fat system is characterized by β_2' crystals at lower T_c and β_2 at higher T_c under static conditions. HS samples are mainly characterized by α and β_2 crystals at lower T_c and α and β_1 crystals at higher T_c when crystallized under dynamic conditions; while the same fat is characterized by β_1' crystals when crystallized at lower T_c and α when crystallized at higher T_c under static conditions after 90 min at T_c. These different polymorphic behaviors, in combination with the different processing and tempering temperatures are translated in different textures in the samples.

Acknowledgments This work was supported by the National Agency for the Promotion of Science and Technology (ANPCyT) of Argentina through Project PICT 0060. The authors wish to thank to the Synchrotron Light National Laboratory (LNLS, Campinas, Brazil) for the use of X-ray facilities through Project D11A-SAXS1-12411.

References

1. O'Brien RD (2009) Fats and oils processing. In: Fats and oils: formulating and processing for applications, Chap 2, CRC Press, NY, pp 73–196
2. Bootello MA, Garces R, Martinez-Force E, Salas JJ (2011) Dry fractionation and crystallization kinetics of high-oleic high-stearic sunflower oil. J Am Oil Chem Soc 88:1511–1519
3. Salas JJ, Bootello MA, Martinez-Force E, Garces R (2011) Production of stearate-rich butters by solvent fractionation of high stearic-high oleic sunflower oil. Food Chem 124:450–458
4. Bootello MA, Hartel RW, Garces R, Martinez-Force E, Salas JJ (2012) Evaluation of high oleic-high stearic sunflower hard stearins for cocoa butter equivalent formulation. Food Chem 134:1409–1417
5. Martini S, Herrera ML, Hartel RW (2001) Effect of cooling rate on nucleation behavior of milk fat-sunflower oil blends. J Agric Food Chem 49:3223–3229
6. Martini S, Herrera ML, Hartel RW (2002) Effect of processing conditions on microstructure of milk fat fraction/sunflower oil blends. J Am Oil Chem Soc 79:1063–1068
7. Martini S, Herrera ML, Hartel RW (2002) Effect of cooling rate on crystallization behavior of milk fat fraction/sunflower oil blends. J Am Oil Chem Soc 79:1055–1062
8. Herrera ML, Hartel RW (2000) Effect of processing conditions on crystallization kinetics of a milk fat model system. J Am Oil Chem Soc 77:1177–1187
9. Herrera ML, Hartel RW (2000) Effect of processing conditions on physical properties of a milk fat model system: rheology. J Am Oil Chem Soc 77:1189–1195
10. Herrera ML, Hartel RW (2000) Effect of processing conditions on physical properties of a milk fat model system: microstructure. J Am Oil Chem Soc 77:1197–1204
11. Rincón-Cardona JA, Martini S, Candal RJ, Herrera ML (2013) Polymorphic behavior during isothermal crystallization of high stearic high oleic sunflower oil stearins. Food Res Int 51:86–97
12. American Oil Chemists' Society (1993) Official method and recommended practices of the American oil chemists' society. Method Cc 1–25: melting point capillary tube method. AOCS, Champaign

13. Martini S, Suzuki AH, Hartel RW (2008) Effect of high intensity ultrasound on crystallization behavior of anhydrous milk fat. J Am Oil Chem Soc 85:621–628. doi:10.1007/s11746-008-1247-5
14. Kaufmann N, De Graef V, Dewenttinck K, Wiking L (2012) Shear-induced crystal structure formation in milk fat and blends with rapeseed. Food Biophys 7:308–316
15. Chaleepa K, Szepes A, Ulrich J (2010) Dry fractionation of coconut oil by melt crystallization. Chem Eng Res Des 88:1217–1222
16. Narine SS, Humphrey KL (2004) A comparison of lipid shortening functionality as a function of molecular ensemble and shear: microstructure, polymorphism, solid fat content and texture. Food Res Int 37:28–38